ORIGINAL ARTICLE

Plant, Cell &
Environment

PCE WILEY

# Natural diversity uncovers *P5CS1* regulation and its role in drought stress tolerance and yield sustainability in barley

Asis Shrestha[1] | Alexander Fendel[1] | Thuy H. Nguyen[2] | Anteneh Adebabay[1] | Annika Stina Kullik[1] | Jan Benndorf[1] | Jens Leon[1] | Ali A. Naz[1]

[1]Department of Plant Breeding, Institute of Crop Science and Resource Conservation, University of Bonn, Bonn, Germany

[2]Department of Crop Science, Institute of Crop Science and Resource Conservation, University of Bonn, Bonn, Germany

**Correspondence**
Ali Ahmad Naz, Department of Plant Breeding, Institute of Crop Science and Resource Conservation, University of Bonn, Bonn, Germany.
Email: a.naz@uni-bonn.de

**Present address**
Asis Shrestha, Quantitative Genetics and Genomics of Plants, Heinrich-Heine-Universität, Düsseldorf, Germany.

Ali A. Naz, Plant Breeding, Faculty of Agricultural Sciences and Landscape Architecture, University of Applied Sciences Osnabrueck, Germany.

## Abstract

Proline accumulation is one of the major responses of plants to many abiotic stresses. However, the significance of proline accumulation for drought stress tolerance remains enigmatic in crop plants. First, we examined the natural variation of the pyrolline-5-carboxylate synthase (*P5CS1*) among 49 barley genotypes. Allele mining identified a previously unknown allelic series that showed polymorphisms at 42 *cis*-elements across the *P5CS1* promoter. Selected haplotypes had quantitative variation in *P5CS1* gene expression and proline accumulation, putatively influenced by both abscisic acid-dependent and independent pathways under drought stress. Next, we introgressed the *P5CS1* allele from a high proline accumulating wild barley accession ISR42-8 into cultivar Scarlett developing a near-isogenic line (NIL-143). NIL-143 accumulated higher proline concentrations than Scarlett under drought stress at seedling and reproductive stages. Under drought stress, NIL-143 showed less pigment damage, sustained photosynthetic health, and higher drought stress recovery compared to Scarlett. Further, the drought-induced damage to yield-related traits, mainly thousand-grain weight, was lower in NIL-143 compared with Scarlett in field conditions. Our data uncovered new variants of the *P5CS1* promoter and the significance of the increased proline accumulation regulated by the *P5CS1* allele of ISR42-8 in drought stress tolerance and yield stability in barley.

**KEYWORDS**
barley, drought tolerance, P5CS1, proline

## 1 | INTRODUCTION

Drought stress is one of the major threats to global agriculture and crop production. The frequency and intensity of dry periods will increase due to decreased precipitation and increased evaporation on a global scale (Hari et al., 2020; Trenberth et al., 2014). Over the last four decades, around 75% of arable land experienced a drought-related yield deficit. The yield of major cereal crops like wheat, barley and maize was particularly affected (Kim et al., 2019). This scenario demands concerted efforts to develop new drought-tolerant varieties in important food crops to face the current and future challenges of climate change.

Water stress targets several physiological processes and leads to reduced photosynthesis (Muzammil, Shrestha, et al., 2018), oxidative

stress (Mittler, 2002), and arrested growth (Barnabás et al., 2008), which ultimately causes yield loss (Chaves & Davies, 2010). Land plants have evolved several morphological, physiological and molecular mechanisms to cope with water stress (Bartels & Sunkar, 2005; Nakashima et al., 2009). One of the widespread tolerance mechanisms across animal and plant species is the accumulation of nontoxic compatible solutes such as proline, soluble sugars, glycine betaine and low molecular weight organic acids (Hochberg et al., 2013; Trovato et al., 2021). The primary role of compatible solutes is to maintain the tissue turgidity and protect the macromolecules in dehydrating cells. Among the compatible solutes, the accumulation of proline is one of the most apparent responses of plants to drought stress (Szabados & Savouré, 2010). Proline primarily facilitates osmotic adjustment and cell membrane stability in stressed tissues (Kavi Kishor et al., 2005; Verslues & Sharp, 1999). Furthermore, proline metabolism might play a role in cellular homeostasis by maintaining the nicotinamide adenine dinucleotide phosphate (NADPH):NADP$^+$ ratio in chloroplasts (Sharma et al., 2011). Previous studies showed that endogenous proline accumulation and exogenous proline application during osmotic stress contribute to reduced oxidative damage and improved biomass production (Hassine et al., 2008; Sripinyowanich et al., 2013; Székely et al., 2008). Besides stress tolerance, adenosine triphosphate synthesized as a result of proline degradation (Kiyosue et al., 1996) can act as an energy source to facilitate stress recovery (Nounjan & Theerakulpisut, 2012; Singh et al., 2000).

Although proline is one of the most studied metabolites and its regulation is established in Arabidopsis, its utility and genetic regulation remain elusive, especially in economically important crops. Previously, we identified a quantitative trait loci (QTL) associated with drought-inducible proline accumulation on chromosome 1 (*QPro.S42-1H*) of barley (Muzammil, Shrestha, et al., 2018). Positional cloning of this QTL allele using a high-resolution population derived from a QTL-bearing introgression line (IL) S42IL-143 identified a novel pyrroline-5-carboxylate synthase (*P5CS1*) allele originated from wild barley ISR42-8 (Muzammil, Shrestha, et al., 2018). Therefore, the objectives of the present study were (1) to identify the natural variation of the *P5CS1* promoter in diverse barley genotypes, (2) to understand the role of the *P5CS1* gene expression on drought stress physiology, and (3) to demonstrate its significance in yield sustainability in field conditions under drought stress.

## 2 | MATERIALS AND METHODS

### 2.1 | Plant material

For allele mining of the promoter region of the *P5CS1* gene, we used 49 barley genotypes comprised of cultivars, landraces and wild barley (Supporting Information: Table S1). We use a German spring barley cultivar Scarlett and a near-isogenic line (NIL) for drought experiments inside climate chamber and field conditions. A NIL was developed by marker-assisted backcrossing with S42IL-143 using

Scarlett as a recurrent parent for three generations (BC$_6$). S42IL-143 was the highest proline accumulating IL under drought conditions among all the ILs of the S42IL mapping population (Muzammil, Shrestha, et al., 2018) and carried the *P5CS1* allele from wild barley ISR42-8 in Scarlett background. Foreground selection was performed using a marker tightly linked to the *P5CS1* gene in the form of a 40 bp insertion/deletion at the 3-untranslated region described in Muzammil, Shrestha, et al. (2018). The NIL is referred to as NIL-143 in the following chapters. Selfing generations two and three of NIL-143 were used to evaluate physiological and yield-related characteristics.

### 2.2 | Allele mining of the *P5CS1* promoter in a barley

We sequenced the *P5CS1* promoter (around 1450 bp upstream of the start codon) in 49 barley genotypes (Supporting Information: Table S1). Next, we performed in silico promoter analysis to predict *cis*-acting elements using plant promoter analysis navigator (Plant-PAN 3.0) and plant *cis*-acting regulatory DNA elements (PLACE) databases. To investigate the proline accumulation and gene expression of *P5CS1*, seeds of five barley genotypes were pregerminated using a peat-based potting mixture (ED73 classic produced and marketed by Einheitserde, einheitserde.de, Germany). Two-day-old seedlings were transferred to 0.5 L pots filled with an equal volume of the potting mixture containing 60% natural sand and 40% topsoil (Terrasoil; Cordel and Sohn). The dry weight and the gravimetric water relations for soil used in the experiment are reported in Supporting Information: Table S2. Plants were grown in an automated climate chamber (Nessler+Esser GmbH and Co.) with 14/10 h light/dark period, 60% relative humidity, 20/18°C day–night temperature, and 100–160 μmol m$^{-2}$s$^{-1}$ light intensity. The field capacity of the soil was maintained at 80% under well-watered conditions before drought stress. Drought stress was applied by withholding watering to 14-day-old seedlings (BBCH 12) for 9 days. All pots under drought stress were weighed manually twice a day to ensure that the reduction of moisture content was at the same level across all the pots. The pots were supplemented with additional water (if needed) to match the highest recorded field capacity among the pots under drought treatment. Control pots were always watered to 80% field capacity. The field capacity of the pots under drought stress reached 31.5± 2.7% 9 days after the start of stress treatment. Shoot samples were harvested 9 days after drought treatment. The samples were snap-frozen in liquid nitrogen and stored at −80°C before proline determination and messenger RNA (mRNA) extraction was done from the ground shoot samples. The experiment was performed in eight biological replicates using a completely randomized design.

Due to the natural variation for the *P5CS1* promoter, we measured shoot proline content in HOR9840, Scarlett, and S42IL-143 under abscisic acid (ABA) treatment. HOR9840 was mainly selected because it carried a deletion allele at coupling element 3 (CE3), one of the components of the ABA response complex (Shen

et al., [1996]) composed of ACGT motifs, CE3 and CE1, in the vicinity. First, 2-day-old seedlings (three seedlings per genotype per tube as technical replicate) were wrapped in a brown-colored germination paper slightly above the crown. Then, the seedlings were placed in 50 ml centrifuge tubes filled with 10 ml 0.5× Hoagland solution (pH 6.0). We exchanged fresh nutrient solution (10 ml) every second day. To prevent hypoxia, we designed the growing setup such that the roots of barley seedlings were not immersed inside the solution and absorbed water and nutrients from the wet germination paper (Supporting Information: Figure S1). After 7 days, seedlings were transferred to 50 ml centrifuge tubes with 10 ml 0.5× Hoagland solution (pH 6.0) containing 50 μM ABA. The nutrient solution was exchanged every 24 h during ABA treatment. The control plants were continually grown in a nutrient solution without ABA. The seedlings were harvested, frozen in liquid nitrogen and stored at −80°C before further processing. The gene expression of putative barley ABF transcription factor (HORVU6Hr1G080670), orthologous to Arabidopsis *ABF1*, was estimated 24 h after ABA treatment for validation of treatment success. In addition, leaf proline content was measured after 24, 48, 72 and 96 h of ABA treatment. The experiment was performed in four biological replications with three technical replicates.

## 2.3 | Evaluation of NIL-143 and Scarlett for drought stress tolerance at the seedling stage

The growing condition and soil type were the same as described above in the allele mining section. The moisture content of the pots under control conditions was maintained at 70% field capacity. Two-week-old seedlings (BBCH 12) under drought stress underwent controlled dehydration, as described earlier. In addition, a series of physiological and biochemical traits were evaluated 4, 5, 6 and 8 days after the start of stress treatment. The moisture content of the pots was $52.1 \pm 4.0\%$, $36.9 \pm 2.0\%$, $26.9 \pm 1.5\%$ and $15.5 \pm 1.1\%$ at 4, 5, 6 and 8 days after the start of stress treatment. The experiment was performed in five biological replicates following a completely randomized design.

### 2.3.1 | Electrolyte leakage (EL) and relative water content (RWC) measurement

Cell membrane integrity was determined by evaluating EL. Fifteen millilitres centrifuge tubes (Falcon®) were filled with 10 ml deionized water and initial electrical conductivity was recorded (ECi). First, we removed the tip (around 2 cm) of the first fully expanded leaf from the top. Then two leaf sections (around 2 cm each) were cut, placed in the centrifuge tubes filled with 10 ml of deionized water, and stored in the dark at room temperature. Electrical conductivity was measured 24 h after the start of the rehydration period (ECf). After the final reading, the samples were boiled at 100°C for 30 min and cooled to room temperature to estimate the total electrical

conductivity (ECt). EL was expressed as (ECf−ECi)/(ECt−ECi) × 100. Leaf water status was estimated through RWC. For RWC measurement, four leaf sections (around 2 cm each) were detached from the first fully expanded leaf, and the fresh weight was recorded (FW). Then, the leaf sections were dipped in a 15 ml centrifuge tube filled with 10 ml of deionized water for 24 h at room temperature. The leaf sections were removed from the tube, and excess water was wiped with a paper towel before taking the turgor weight (TW). Dry weight was recorded after oven drying at 70°C for 72 h. RWC was estimated as (FW−DW)/(TW−DW) × 100.

### 2.3.2 | Malondialdehyde (MDA) determination

Oxidative damage of lipid membrane during drought stress was estimated by determining MDA concentration using the thiobarbituric acid (TBA) method adapted to a microplate-based protocol (Dziwornu et al., [2018]). Shoot samples were homogenized in liquid nitrogen, and MDA was extracted using 1.5 ml of 0.1% trichloroacetic acid (TCA), followed by centrifuging at 14 000*g* for 15 min at 4°C. Then, 500 μl supernatant was mixed with reaction solution I (0.01% 2,6-di-tert-butyl-4-methyl phenol (BHT) in 20% TCA) and reaction solution II (0.65% TBA, 0.01% BHT in 20% TCA) in a 1:1 ratio in separate 15 ml centrifuge tubes. The reaction and sample mix were incubated at 95°C for 30 min. After incubation, the reaction was stopped on ice for 5 min and the reaction mix was centrifuged at 8000*g* for 10 min at 4°C. The absorbance was measured at 440, 532 and 600 nm using a microplate reader (TECAN Infinite 200 Pro; TECAN Group Limited). MDA concentration was expressed as nanomoles per gram of fresh weight.

### 2.3.3 | Evaluation of vegetation indices (VIs) and photosynthetic parameters

VIs were recorded using portable spectrometric devices like the chlorophyll meter (SPAD-502Plus; Konica Minolta) and photon system instrument (PolyPen RP 410; PSI) using manufacturer instructions. Supporting Information: Table S3 contains the description of the VIs used in the study. VIs were scored from 4 to 8 days after the drought stress treatment started. The measurements were made in the first fully expanded leaves from the top.

Gas exchange measurement was performed using a portable photosynthesis system (LI-6400 XT gas exchange analyzer; LI-COR Biosciences) after 4, 6 and 8 days after the drought stress treatment started. The measurements were made in the first fully expanded leaves from the top. The $A/C_i$ curve measurement was performed in the middle part of the leaf inside a leaf chamber. The parameters inside the leaf chamber were set as constant photosynthetic active radiation of $1500 \, \mu mol \, m^{-2} \, s^{-1}$, relative humidity of approximately 52%, and temperature corresponding to leaf temperature and flow rate at $300 \, \mu mol \, s^{-1}$. The gas exchange was measured by supplying external $CO_2$ at varying concentrations (400, 300, 200, 250, 100, 50,

400, 600, 800, 1000, 1200, 1400 and 1600 ppm). The infrared gas exchange analyzer automatically logs the photosynthetic parameters, including the rate of $CO_2$ assimilation ($A$), intercellular $CO_2$ ($C_i$), stomatal conductance ($g_s$), and transpiration rate ($E$). $A/C_i$ curve was plotted to estimate the maximum carboxylation rate of Rubisco ($V_{cmax}$) and the maximum rate of electron transport during ribulose-1,5-biphosphate regeneration ($J_{max}$) using a nonlinear fitting program according to (Sharkey et al., 2007, 2016). The estimated $V_{cmax}$ and $J_{max}$ were then adjusted to a temperature of 25°C for data presentation. In addition, the effective quantum yield of photosystem II (Y(II)) at steady-state photosynthesis under light conditions was determined using MiniPam (MINI-PAM-II; Heinz Walz).

### 2.3.4 | Proline determination

Proline was measured from shoot samples, according to Bates et al. (1973), adapted to a microplate-based protocol (Abrahám et al., 2010). In short, seedlings were homogenized in liquid nitrogen, and proline was extracted using 1 ml 3% sulphosalicylic acid. The extract was centrifuged at 12 000$g$ for 5 min. The supernatant was incubated for 1 h at 96°C with 2.5% ninhydrin and acetic acid at a 1:1:1 ratio. The reaction was stopped on ice, and the proline-ninhydrin reaction product was extracted with 1 ml toluene. The absorbance of chromatophore-containing toluene was measured at 520 nm using a microplate reader (TECAN Infinite 200 Pro; TECAN Group Limited). Shoot proline level was determined using a standard curve method and expressed as micrograms per gram of fresh weight ($\mu g\,g^{-1}$ FW).

### 2.4 | mRNA expression analysis using quantitative real-time polymerase chain reaction (PCR)

RNA was extracted in three biological replicates from control and treatment samples from allele mining and drought experiments at the seedling stage. The RNA concentration and quality were determined by running on 1% Agarose gel and nanodrop (NanoDrop 2000c; Thermo Fischer Scientific) before complementary DNA (cDNA) synthesis. cDNA was synthesized using the Revertaid H-minus cDNA synthesis kit (Thermo Fischer Scientific) following the manufacturer's instruction. An SYBR green-based qPCR master mix (Thermo Fischer Scientific) was used in the assay with three technical replicates per sample. The quantitative polymerase chain reaction (qPCR) run was set to initial denaturation at 95°C for 3 min, followed by 40 cycles (95°C for 15 s, 60°C for 1 min). Specific amplification was analyzed using a melt curve (95°C for 15 s, 60°C for 1 min, 95°C for 15 s). Relative mRNA expression of target genes was calculated based on the $2^{-\Delta\Delta C_t}$ method (Livak & Schmittgen, 2001). Elongation factor-beta was used as the reference gene for relative quantification. The primers used in the qPCR assay (efficiency of more than 88%) are provided in Supporting Information: Table S4.

### 2.5 | Evaluation of stress recovery at the seedling stage in the greenhouse

Two-day-old seedlings of Scarlett and NIL-143 were transferred to a 1 L capacity pot filled with a potting mixture of 60% natural sand and 40% topsoil (Terrasoil; Cordel and Sohn). All the pots were filled with an equal amount of soil (975 g on a dry weight basis), and the moisture level was maintained at 70% field capacity. The plants were grown in the greenhouse, and the growing condition was 18–22°C daily mean temperature. Fifteen seedlings were grown in one pot for 12 days (BBCH 12), and the pots were dehydrated by withholding watering. Twelve days after the start of dehydration (6.9 ± 2.1% field capacity), the pots were rewatered, and we recorded the number of seedlings that were able to survive 1 week after rehydration. The recovery rate was calculated by counting the number of seedlings that formed true leaves after rehydration. The experiment was performed three times at intervals of 2 weeks between experiments. NIL-143 and Scarlett were grown in separate pots in the first two repetitions. Five pots of each genotype were evaluated per experimental repetition. In the third experiment, the results were further confirmed by repeating the same experiment where NIL-143 and Scarlett were grown in a single pot.

### 2.6 | Evaluation of adaptive traits under drought stress in field conditions

The reproductive and physiological performance of NIL-143 and Scarlett was evaluated in a field condition in Campus Klein-Altendorf (50°37′ N, 6°59′ E) in the year 2019 and 2020. In a randomized complete block design, a row experiment was implemented inside a rainout shelter in 2019. Three plots were prepared for the experiment, two inside the rainout shelter (drought and irrigated) and one outside under rainfed conditions. Each plot was divided into five blocks and the size of each block was 40 cm × 120 cm. One block constituted six rows. Outer two rows were treated as the border while NIL-143 and Scarlett were sown in the inner four rows. Twenty kernels per genotype were sown in each row at a spacing of 2 cm. The distance between the rows was 20 cm (250 seeds/m²). Therefore, there were ten rows each for NIL-143 and Scarlett for every growing condition. The plots were watered with automated overhead sprinklers watering at approximately 5 mm/day in soil type characterized as Haplic Luvisol (Koua et al., 2021).

Volumetric moisture content (VMC) was measured using a data logger M50 Data Logger (ICT International) installed at a depth of 0–10 cm. Irrigation was stopped in the drought plot before the heading stage (BBCH 41) for 3 weeks until the VMC reached 5%. The weather and moisture data are presented in Supporting Information: Figure S2. Fertilizer application and plant protection measures were followed as described in Siddiqui et al. (2021). We scored VIs and Y (II) as described earlier at 7, 14 and 21 days after the start of drought stress treatment. The data were collected from the second fully expanded leaf (one leaf below the flag leaf) from three plants in the middle of each row. The second fully expanded leaf from the top was harvested 14 days after a drought for proline determination. In addition, photosynthetic health was

determined by measuring Y (II) using MiniPam. Matured ears and straw were harvested and oven-dried at 30°C and 70°C for 72 h before evaluating the yield-related characteristics. During manual harvesting, we bulked all the ears and straw from a single row. Grain weight, shoot biomass, tiller numbers, and ear numbers from the row were averaged across the number of plants, and the values are expressed as per plant.

In 2020, a mini yield plot experiment was carried out again in the rainout shelter and rainfed conditions in a randomized complete block design. Each growing condition contained two blocks with six mini-plots (3 m × 0.5 m). Within a block, NIL-143 and Scarlett were sown in three mini-plots with a sowing density of 200 seeds/m². Therefore, every growing condition constituted six mini-plots per genotype (three per block). Irrigation, drought stress treatment, fertilizer application and plant protection measures were applied according to the row experiment performed in 2019. After maturity, the plots were harvested using a combined harvester. We estimated grain yield per plot and thousand-grain weight in 2020.

## 2.7 | Statistical analyses

Data processing and statistical significances were analyzed using open-access statistical computing software R version R.3.6.3 (R Core Team, 2020). We used the output of the quantile-quantile plot using R package ggpubr to check if the data followed normal or close to normal distribution. A three-way analysis of variance (ANOVA) was performed to estimate the genotype, treatment and genotype by treatment interaction effects for the data obtained from physiological and spectral measurements during the seedling stage and external ABA application. Similarly, a four-way ANOVA was performed to evaluate the genotype, treatment, block and genotype by treatment interaction effects for the data obtained from the field experiments.

The statistical analysis for leaf proline concentration and relative expression data was done after $log_{10}$ transformation of the original observation. Next, we performed a one-way ANOVA followed by multiple mean comparisons using the Tukey test (post hoc test) when the experiments involved more than two genotypes in evaluating within treatment genotypic differences. For the experiments with only two genotypes, the genotypic mean within treatment was compared using a student's t-test. Finally, for correlation analysis, the adjusted entry means of genotypes for a treatment level were obtained across the different days of data collection. The graphics were prepared using R and Prism8.

## 3 | RESULTS

### 3.1 | Allele mining of the P5CS1 promoter identified promoter variation associated with differences in drought-inducible proline accumulation

We analyzed the promoter region of the P5CS1 gene in 49 barley genotypes. The conserved motif prediction tools (PlantPan 3.0) identified 130 cis-acting elements in the P5CS1 promoter from ISR42-8 (Supporting Information: Table S5). The commonly occurring motifs were ABA-responsive factors binding elements (ABRE) and related coupling elements (CE), MYB binding motifs, CGACGOSA-MY3, CACTFTPPCA1, CGCGBOXAT, CAATBOX1 and HEXAMER-ATH4. In addition, NAC binding motifs, WRKY binding motifs, and dehydration responsive elements (DRE) were also detected in the P5CS1 promoter (Supporting Information: Table S5). We found allelic series across 42 cis-acting elements (Supporting Information: Table S5), and the sequence variations across those motifs were used to perform principal component analysis. The first principal component separated a wild barley HOR 2514, three landraces (BCC282, NGB4605 and HOR2448), and a cultivar BCC848 from the rest of the genotypes (Supporting Information: Figure S3A). The second and third principal components separated wild barley HOR9840 and ISR42-8 from other genotypes, respectively (Figure S3A,B). The polymorphisms detected across the cis-acting elements have not been reported in other studies on natural variation of the P5CS1 locus (Xia et al., 2017). For example, a cluster of ABRE and related coupling elements were located close to each other, around 1.4 kb upstream of the start codon of P5CS1. Although the core motif of the ACGT box was conserved in that region, indels and single-nucleotide polymorphisms (SNPs) were detected on the core sequence of coupling elements. Only ISR42-8 carried an entire core sequence of CE1 (CACCG), while other genotypes had A/G substitution at the locus. One of the genotypes, HOR9840, carried a 10 bp deletion allele, which resulted in a loss of predicted CE3 in that region. Likewise, 130 bp deletions in HOR2514, NGB4605, HOR2448, BCC282 and BCC848 resulted in a loss of 14 predicted motifs, including ABRE and MYB binding motifs (Supporting Information: Table S5, Figure S4, and Figure 1a).

We selected five genotypes representing different clusters based on the principal component analysis to test if promoter variation correlates with proline accumulation. We observed significant genotype, treatment and genotype by treatment interaction for shoot proline content and P5CS1 expression (Supporting Information: Table S6). Shoot proline level was highest in ISR42-8, while HOR9840, which had polymorphisms across multiple (15) DNA binding domains, accumulated the lowest proline under drought stress, with proline concentrations around six-fold lower in HOR9840 than ISR42-8 (Figure 1b). A spring barley cultivar Scarlett and a landrace NGB4605 accumulated similar proline levels. The proline accumulation in another wild barley ICB181160 was intermediate between HOR9840 and Scarlett. Then, we checked the gene expression of P5CS1 using qPCR. Gene expression of P5CS1 was lowest for HOR9840 and highest for ISR42-8 (Figure 1c). Overall, the expression of P5CS1 correlated with shoot proline concentration ($R^2 = 0.81$). Apart from this, the number of the polymorphic predicted motifs was lowest in ICB181160 (9) compared to NGB4605 (20), HOR9840 (15) and Scarlett (10). However, the proline content in ICB181160 under drought was slightly higher than HOR9840 and lower than NGB4605 (Figure 1a,b). Therefore, some motifs might be more critical than others, or variation exists in upstream regulators that target the P5CS1 promoter region.
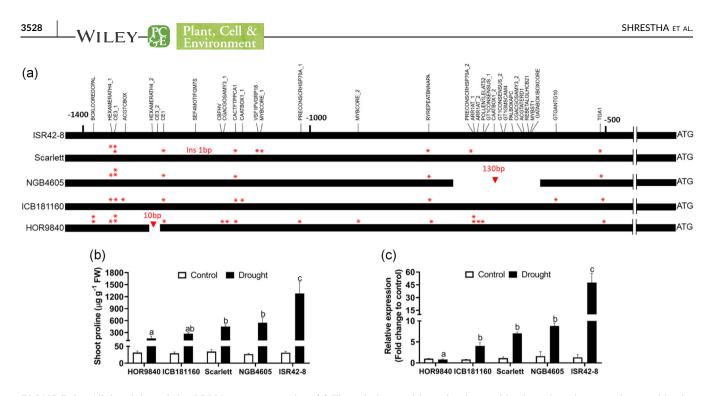
**FIGURE 1** Allele mining of the *P5CS1* promoter region. (a) The relative position of polymorphic *cis*-acting elements detected in the *P5CS1* promoter. Asterisks indicate the number of single nucleotide polymorphisms detected across the *cis*-elements. Triangle indicates the site of deletions. The core sequence and the allelic differences of the indicated motifs can be found in Supporting Information: Table S5 and Figure S4. (b) Shoot proline concentration in five barley genotypes grown inside an automated climate chamber. Bars represent mean + SE (*n* = 8). (c) Gene expression of *P5CS1*. FW, fresh weight. Bars represent mean + SE (*n* = 3). Indexed letters above the bars indicate significant differences between the genotypes ($p \leq 0.05$), not sharing the same letter under drought conditions using the Tukey's test. The statistical analysis was performed on $\log_{10}$ transformed data of the original observations.

Because we observed a deletion allele in the ABA response complex (Shen et al., 1996) in HOR9840, we selected HOR9840, Scarlett, and S42IL-143 to evaluate the response of proline accumulation to external ABA application. The expression of the barley ortholog of *ABF1* increased by three- to four-fold in all the genotypes 24 h after ABA application, indicative of treatment success (Supporting Information: Figure S5A) with no genotypic difference for the gene expression (Supporting Information: Table S7). In contrast, HOR9840 accumulated the lowest and S42IL-143 accumulated the highest shoot proline in response to ABA application (Supporting Information: Figure S5B and Table S7). To summarize, allele mining identified previously undescribed variations in the *cis*-acting element of the *P5CS1* promoter, especially across ABRE, MYB binding motifs, HEXAMERATH4, CGACGOSAMY3. Consistent with this, the genotypes also differed in ABA-induced proline accumulation.

## 3.2 | NIL-143 accumulates more proline than cultivar Scarlett under drought stress conditions

NIL-143 is a near-isogenic line where *QPro.S42-1H* from wild barley accession ISR42-8 is introgressed into Scarlett. *QPro.S42-1H* is a QTL controlling drought-inducible proline accumulation in

barley (Muzammil, Shrestha, et al., 2018). Therefore, we estimated the proline accumulation in the seedlings of Scarlett and NIL-143 at 4, 5, 6 and 8 days after the start of drought stress treatment. We observed a significant treatment effect 5 days after stress treatment (Supporting Information: Table S8). However, compared to control conditions, the proline accumulation increased only in NIL-143 5 days of drought stress (Supporting Information: Table S8). The proline level in NIL-143 was 2 to 2.5-fold higher than in Scarlett under drought stress. The shoot proline content did not differ between NIL-143 and Scarlett under control conditions (Figure 2a). Furthermore, the *P5CS1* expression was around 1.5- and 2-fold higher in NIL-143 compared to Scarlett (Figure 2b).

In addition, we analyzed the expression of barley ortholog of other proline metabolism genes identified in Arabidopsis, namely, *P5CR*, *PDH* and *P5CDH*. We found a single blast hit sharing high homology with these genes in barely Morex reference (Supporting Information: Table S4). *P5CR* and *P5CDH* expression was induced upon drought treatment, while the expression of *PDH* was suppressed under drought stress. However, none of these proline metabolism genes differed in expression between NIL-143 and Scarlett (Figure 2c–e). Taken together, the onset of proline accumulation occurred earlier and proline accumulated to higher levels in NIL-143 compared with Scarlett.
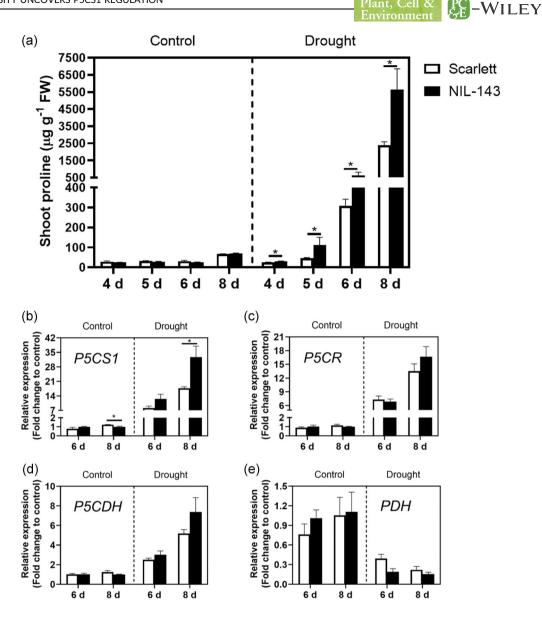
**FIGURE 2** Proline accumulation in NIL-143 and Scarlett at the seedling stage in response to drought stress grown inside an automated climate chamber. Drought treatment was applied to 2-week-old seedlings by terminating the water supply. Sampling was done at 4, 5, 6 and 8 days after the start of drought stress treatment. (a) Shoot proline concentration under control and drought conditions. The graph represents the mean + SE ($n$ = 5). Asterisks indicate significant differences between genotypes (*$p \leq 0.05$) using a student's $t$-test. (b–e) Effect of drought stress on the expression of (b) *P5CS1* (c) *P5CR* (d) *P5CDH* (e) *PDH* genes 6 and 8 days after the start of drought stress treatment. FW, fresh weight. The graph represents the mean + SE ($n$ = 3). Asterisks indicate significant differences between genotypes (*$p \leq 0.05$). The statistical analysis was performed on $\log_{10}$ transformed data of the original observations.

## 3.3 | NIL-143 displayed improved drought stress tolerance and stress recovery at the seedling stage

To gain insight into the effect of *QPro.S42-1H* on the physiological adjustment to drought stress, we evaluated tissue hydration status, membrane stability, and oxidative stress in NIL-143 and Scarlett. We observed a significant effect of drought treatment on EL, MDA levels and RWC of leaf tissues (Supporting Information: Table S8). For instance, the extent of membrane damage estimated as EL rose by around 1.2 and 2-fold higher in Scarlett than NIL-143 at 6 and 8 days after drought stress, respectively (Figure 3a). RWC was significantly

reduced in both lines 6 days after drought stress treatment, but the values were not statistically significant between NIL-143 and Scarlett (Figure 3b). In addition, shoot MDA content was lower in NIL-143 compared with Scarlett 8 days after drought stress treatment (Figure 3c).

The evaluation of VIs is a popular method applied to assess plant health under different growing conditions. We observed a significant decrease in VIs in plants exposed to drought stress compared to plants under control conditions (Supporting Information: Table S8). One of the most commonly used indices, normalized difference vegetation index (NDVI), was significantly higher in NIL-143
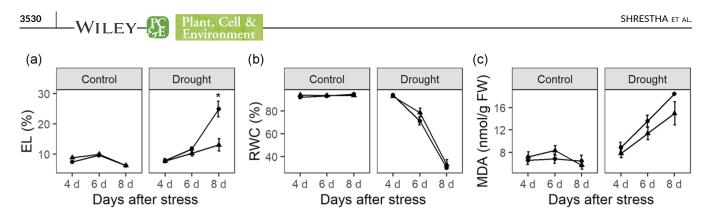
**FIGURE 3** Physiological responses of NIL-143 and Scarlett to drought stress at the seedling stage grown inside an automated climate chamber. Effect of drought on (a) Electrolyte leakage (EL), (b) Relative water content (RWC) of leaf, and (c) Malondialdehyde (MDA) concentration. Drought treatment was applied to 2-week-old seedlings by terminating the water supply. Sampling was done at 4, 6 and 8 days after the start of drought stress treatment to analyze the biochemical and physiological response of plants to drought stress. EL, electrolyte leakage; FW, fresh weight. Bar indicates mean ± SE ($n = 5$). Asterisks indicate significant differences between genotypes (*$p \leq 0.05$, **$p \leq 0.01$).
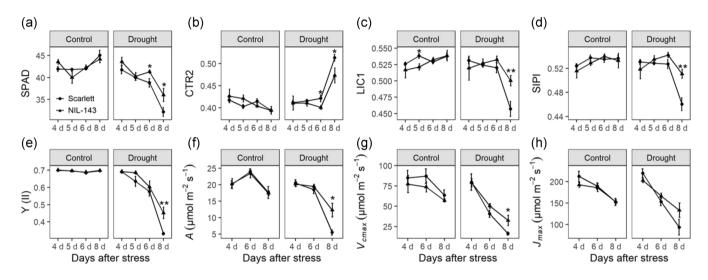


**FIGURE 4** Vegetation indices and photosynthetic traits in NIL-143 and Scarlett under drought stress at the seedling stage grown inside an automated climate chamber. Effect of water stress on (a) soil plant analysis development (SPAD) chlorophyll meter value, (b) Carter index 2 (CTR2), (c) Lichtenthaler index 1 (LIC1), (d) structure intensive pigment index (SIPI), (e) effective quantum yield of photosystem II (Y(II)), (f) net rate of $CO_2$ assimilation (A), (g) maximum carboxylation rate of rubisco ($V_{cmax}$), and (h) maximum rate of electron transport ($J_{max}$). Drought treatment was applied to 2-week-old seedlings by terminating the water supply. Photosynthesis-related traits were evaluated at 4, 5, 6 and 8 days after the start of drought stress treatment using MiniPam and LI-6400XT gas exchange analyzer. The graph indicates mean ± SE ($n = 5$). Asterisks indicate significant differences between genotypes (*$p \leq 0.05$, **$p \leq 0.01$).

compared to Scarlett at 6 and 8 days after drought stress (Supporting Information: Figure S6A). Similarly, SPAD, simple ratio (SR) index, simple ratio pigment index (SIPI) and Lichtenthaler index (LIC1) significantly decreased in Scarlett compared to NIL-143 plants under drought stress conditions (Figure 4a,c,d; Supporting Information: Figures S6B,C). Carter index 2 (CTR2) revealed a different trend as the values increased in plants grown under drought stress compared to well-watered plants and CTR2 values were significantly higher in Scarlett at 6 and 8 days after the start of stress treatment than NIL-143 (Figure 4b).

Next, we examined the photosynthetic health of NIL-143 and Scarlett at different stages of drought to learn the potential benefit of *QPro.S42-1H*. Y(II) declined in stressed plants compared to plants under the control conditions and Y(II) was 9% and 27% more

effective in NIL-143 under drought stress than Scarlett (Figure 4e). Besides, photosynthetic efficiency estimated using an infrared gas exchange analyzer declined under stress conditions. Nevertheless, NIL-143 maintained a higher A and $g_s$ than Scarlett under stress conditions (Figure 4f and Supporting Information: Figure S7A). Furthermore, E was around 31% higher in the stressed plants of NIL-143 than in Scarlett 8 days after stress treatment (Supporting Information: Figure S7B). In addition, NIL-143 showed 50% and 30% higher $V_{cmax}$ and $J_{max}$ than Scarlett (Figure 4g,h) 8 days after the start of drought stress treatment. We did not detect genotypic differences for photosynthetic traits under control conditions (Figure 4 and Supporting Information: Figure S7).

We performed recovery experiments in the greenhouse to understand the role of *QPro.S42-1H* on the resumption of plant

growth after stress. Two-week-old seedlings grown in pots were dehydrated for 12 days and rewatered to observe the recovery process. Notably, the images recorded 7 days after rewatering indicated a higher recovery rate in NIL-143 compared with Scarlett (Figure 5a–c). After rehydration, one-third of Scarlett seedlings survived, whereas 60% recovery was recorded for NIL-143 seedlings (Figure 5c). Although the pot effect was not statistically significant, we repeated the experiment by growing NIL-143 and Scarlett in single pots to rule out the probable environmental effect. The recovery rate followed a similar trend in the single pot experiment (Supporting Information: Figure S8). Therefore, the introgression of *QPro.S42-1H* into Scarlett improved stress recovery.

## 3.4 | NIL-143 displayed improved drought stress tolerance and yield sustainability under field conditions

To investigate the role of *QPro.S42-1H* from wild barley ISR42-8 on drought tolerance in field conditions, we evaluated the response of NIL-143 and Scarlett to drought stress in a rainout shelter. We maintained two blocks inside the rainout shelter and drought stress was applied for 21 days in one block. The leaf proline content was significantly higher in NIL-143 than Scarlett in irrigated and nonirrigated conditions 14 days after the stress treatment started (Supporting Information: Figure S9). Similar to the growth chamber experiment at the seeding stage, a significant
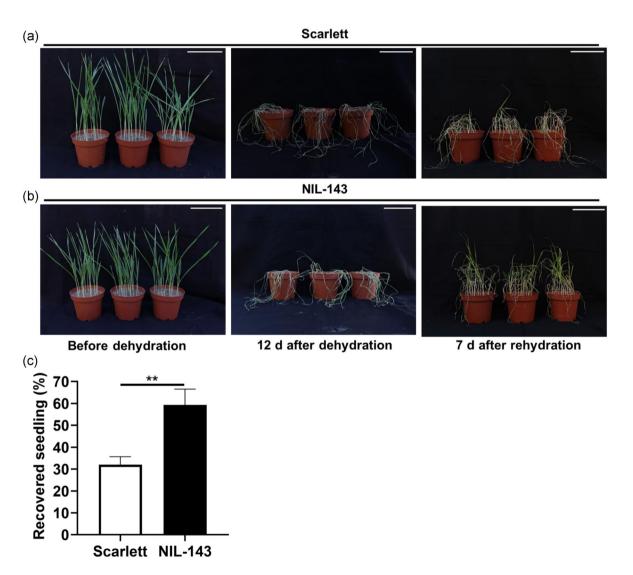


**FIGURE 5** Stress recovery in NIL-143 and Scarlett at the seedling stage greenhouse conditions. Image of representative pots of (a) Scarlett and (b) NIL-143 before the start of dehydration and after rehydration. Fifteen seedlings were grown in a 1 L pot for 14 days at 70% field capacity. Two-week-old seedlings were subjected to dehydration stress by withholding the water supply for 12 days. The images were taken 7 days after rewatering using Canon 750D. (c) The percentage of recovered seedlings was determined by counting the number of plants producing true leaves after rehydration. Scoring was done 14 days after rewatering. The experiment was repeated twice in five biological replicates. The graph represents mean + SE ($n = 10$). Asterisks indicate significant differences between genotypes (**$p \leq 0.01$). White scale bars indicate a width of 12 cm. [Color figure can be viewed at wileyonlinelibrary.com]

treatment effect was observed in Y(II) and VIs in field conditions (Supporting Information: Table S9). Scarlett plants experienced more physiological stress than NIL-143, especially 21 days after drought stress treatment (Figure 6 and Supporting Information: Figure S10). For instance, Y(II) was more than two-fold higher in NIL-143 compared with cultivar Scarlett 21 d after drought stress treatment (Figure 6a). Similarly, NDVI and SPAD values were higher in NIL-143 than in Scarlett, indicating less damage to chlorophyll in NIL-143 (Supporting Information: Figure S10A, Figure 6b).

To determine the contribution of *QPro.S42-1H* on the yield-related performance under stress conditions, we evaluated several yield attributes under control, drought, and rainfed conditions. Both straw biomass and grain yield-related traits were significantly affected by drought stress (Supporting Information: Table S10). Nonetheless, NIL-143 showed superior performance for yield-related traits, including thousand-grain weight and grain weight per plant under drought stress (Figure 7a,b and Supporting Information: Figure S11). Grain weight per plant, grain number per ear, and thousand-grain weight were 35%, 18% and 7% higher in NIL-143
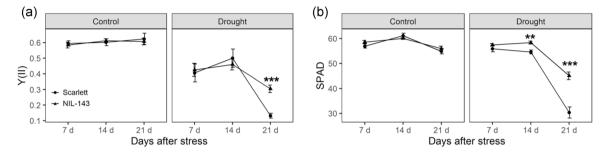


**FIGURE 6** Photosynthetic parameters and vegetation index of NIL-143 and Scarlett in field conditions. Effect of drought stress on (a) effective quantum yield of photosystem II (Y(II)) (b) soil plant analysis development (SPAD) chlorophyll meter value. Scarlett and NIL-143 were grown in 40 cm rows inside a rainout shelter. One plot was regularly irrigated, while drought stress was applied to another plot for 21 days at the heading stage (BBCH 41). Vegetation indexes and photosynthetic traits were scored at 7, 14 and 21 days after the start of stress treatment. The graph indicates mean ± SE ($n = 10$). Asterisks indicate significant differences between genotypes (**$p ≤ 0.01$, ***$p ≤ 0.001$).
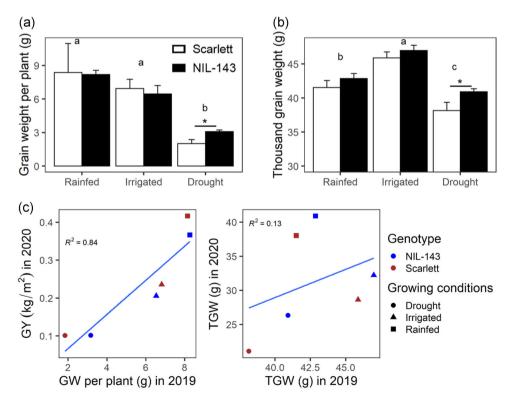


**FIGURE 7** Yield and related traits of NIL-143 and Scarlett under field conditions. Effect of drought stress on (a) grain weight per plant and (b) thousand-grain weight (TGW). The graph represents mean + SE ($n = 10$). Asterisks indicate significant differences between genotypes ($p ≤ 0.05$). The growing conditions not sharing the same letter indicate a significant difference using the Tukey's post hoc test. (c) The correlation between the grain weight (GW) per plant and grain yield (GY) per m$^2$ and thousand-grain weight was evaluated in field experiments in 2019 and 2020. [Color figure can be viewed at wileyonlinelibrary.com]

than in Scarlett under drought stress (Figure 7 and Supporting Information: Figure S11C). Furthermore, the harvest index was higher in NIL-143 than in Scarlett under drought conditions (Supporting Information: Figure S11E). In 2020, we evaluated the grain yield in mini-plots (4.5 m$^2$). We observed a significant treatment and genotype effect for thousand-grain weight and treatment effect for grain yield per m$^2$ (Supporting Information: Table S11). The observations were consistent with the row experiment, as the thousand-grain weight higher in NIL-143 than Scarlett, irrespective of growing conditions (Figure 7b and Supporting Information: Figure S12A). Grain yield per plot was significantly reduced for both NIL-143 (50%) and Scarlett (57%) under drought stress compared to control conditions (Supporting Information: Figure S12B). We also observed a strong positive phenotypic correlation between grain yield per plant in 2019 and grain yield per m$^2$ in 2020 ($R^2 = 0.83$). A weak positive correlation ($R^2 = 0.13$) was observed for thousand-grain weight between 2019 and 2020 because the thousand-grain weight plant was higher in rainfed conditions than in irrigated plots inside the rainout shelter in 2020 in contrast to 2019 (Figure 7c). Overall, the yield data indicated that QPro.S42-1H positively affects barley yield-related characters under stress, especially grain size.

## 4 | DISCUSSION

In a previous study, we identified a possible causative mutation in the promoter of P5CS1 related to drought-inducible proline accumulation in barley (Muzamil, Shrestha, et al., 2018). Therefore, the current study aimed to identify and characterize the natural variation of P5CS1 in diverse barley accessions. In addition, we studied the association between P5CS1 promoter variation and proline synthesis and tested its significance for developing drought-tolerant genotypes. First, we performed allele mining through sequence analysis of the P5CS1 promoter in the barley diversity panel. We identified 42 polymorphic cis-elements across the P5CS1 promote, including motifs targeted by stress-inducible transcription factors such as MYB (Aleksza et al., 2017) and ABF (Yoshida et al., 2015) between ISR42-8 and other genotypes (Supporting Information: Table S5). The most striking difference in proline accumulation compared with ISR42-8 was observed in another wild barley accession HOR9840, with 15 polymorphic cis-acting elements such as ABRE, CE3, CE1, HEXAMERATH4 and MYB binding motifs compared to ISR42-8 (Figure 1a,b). The protein sequence of P5CS1 in ISR42-8 and HOR9840 was identical (Supporting Information: Figure S13), ruling out coding sequence polymorphism as a causative polymorphism for shoot proline content. These results align with the well-established notion that the cooperative action of multiple transcription factors is necessary to transactivate response genes (Biłas et al., 2016).

In addition to drought stress, proline accumulation in response to ABA application was also lowest in HOR9840 compared to S42IL-143 (Supporting Information: Figure S5b). HOR9840 carried a deletion allele and A/G substitution at predicted CE3 and CE1, respectively, around 30 bp downstream of the ACGT box (Figure 1a

and Supporting Information: Figure S4). It has been shown that CE3 might be functionally equivalent to ABRE with ACGT as a core sequence (Hobo et al., 1999). Moreover, multiple ABREs or the combination of an ABRE with one of several non-ACGT ABREs (CE1 and CE3) across the promoter region successfully induced reporter gene expression upon ABA treatment (Shen et al., 1996). Recently, we also reported that ABA-responsive transcription factors contributed to proline synthesis under ABA signaling in Arabidopsis (Shrestha et al., 2021). Although further research is required, it is tempting to claim that the complete loss of CE3 due to 10 bp deletion might be one of the critical promoter variations causing reduced proline accumulation in HOR9840.

Furthermore, the predicted motifs in the P5CS1 promoter revealed the presence of motifs putatively targeted by ABA-dependent and ABA-independent genetic factors. For instance, seven out of ten polymorphic motifs between Scarlett and ISR42-8 were non-ABREs (Figure 1a). This might explain a more substantial variation in the proline induction under drought stress between Scarlett and NIL-143 than ABA treatment (Figure 2a and Supporting Information: Figure S5B). Furthermore, it highlights that ABA-independent pathways are equally crucial for P5CS1 gene expression and subsequent proline accumulation in barley. We also identified four QTL in addition to QPro.S42-1H in a mapping population developed from ISR42-8 and Scarlett (Muzammil, 2018), indicating a more complex inheritance of drought-induced proline accumulation beyond P5CS1 regulation. Therefore, we observed a higher difference in proline accumulation between ISR42-8 and Scarlett (three-fold) than between NIL-143 and Scarlett (2 to 2.5-fold) (Figures 1b and 2a). Likewise, GWAS in Arabidopsis successfully identified genetic loci and candidate genes linked to proline synthesis other than major biosynthetic genes (Verslues et al., 2014). Our next goal is to follow QTLs other than QPro.S42-1H, associated with drought-induced proline synthesis and genome-wide mapping strategies using larger germplasm collections. In addition, more work will be done to experimentally validate the individual SNPs and their role in proline accumulation in barley.

The proline accumulation in ISR42-8 was significantly higher than in other genotypes. Therefore, we developed NIL-143 carrying the P5CS1 allele of ISR42-8 in the Scarlett background. NIL-143 and Scarlett were screened under different growing environments (climate chamber and field conditions) and growth stages (seedling and reproductive) to evaluate the response to water-limited conditions. The leaf proline concentration was lower in Scarlett than NIL-143 under drought stress at the seedling and reproductive stages (Figure 2a and Supporting Information: Figure S9). The proline content was also elevated in the irrigated conditions in the field, which could be attributed to higher atmospheric temperature in the field conditions (Supporting Information: Figure S9). Furthermore, the gene expression of P5CS1 was higher in NIL-143 than in Scarlett under drought stress (Figure 2b). P5CR is involved in reducing P5C to proline and P5CDH transcription is induced to avoid P5C toxicity (Sharma & Verslues, 2010). On the other hand, PDH expression is downregulated under drought stress as a feedback response to

proline accumulation (Sharma et al., 2011). As expected, the gene expression of *P5CR* and *P5CDH* was elevated, while *PDH* expression was reduced in both genotypes under drought stress (Figure 2c–e).

Physiological processes like photosynthesis, degradation of chlorophyll pigment, oxidative stress, and membrane damage are often associated with drought stress (Le Maire et al., 2004). We observed that NIL-143 showed superior membrane integrity and reduced MDA levels under severe drought stress compared to Scarlett (Figure 3a,c). In addition, NIL-143 maintained a higher transpiration rate and a 10% higher RWC (statistically nonsignificant) than Scarlett (Supporting Information: Figure S7B and Figure 3b). Therefore, the membrane integrity might be attributed to molecular chaperone activity of proline on membrane proteins and phospholipid layer (Chattopadhyay et al., 2004; Hare et al., 1998; Rajendrakumar et al., 1994) in NIL-143 than Scarlett under drought stress which warrants further experimentation.

We observed a high correlation between the spectral measurements evaluated in a controlled environment and field conditions (Supporting Information: Figure S14). For example, SPAD values indicated Scarlett incurred more damage to chlorophyll pigments than NIL-143 under stress conditions at the seedling and reproductive stage (Figures 4a and 6b). Other comparable indices like NDVI, SR and RDVI also showed similar responses to drought (Supporting Information: Figures S6 and S10). These VIs are derived from the transmittance ratio of infrared to red (maximum chlorophyll absorption range) light through the leaf surface (Main et al., 2011; Uddling et al., 2007). Furthermore, we also analyzed other VIs based on the ratio of the narrow spectral range, such as LIC1, CTR, SIPI, Gitelson and Merzlyak index 2 (GM2), simple ratio pigment index (SPRI), and Zarco-Tejada and Miller index (ZMI). All other but CTR2 index increased with drought stress, and Scarlett plants under stress displayed the highest CTR2 values (Supporting Information: Table S8 and S9). These results agree with Carter (1994), who showed that the increased value of CTR indexes reflects plant stress. The slow and reduced degradation of photosynthetic pigment in NIL-143 is supported by previous studies where proline accumulation was associated with decreased chlorophyll damage in different plant species (Fedina et al., 2003; Gadallah, 1999; Székely et al., 2008).

The photosynthesis health of NIL-143 was better than Scarlett, indicated by a lower reduction in photosynthetic parameters such as Y(II), $E$, $A$, $V_{cmax}$, and $J_{max}$ under drought stress conditions (Figures 4e–h and 6a). Similar to our observations, a positive correlation between photosynthesis rate and proline accumulation under osmotic stress was reported before (Hassine et al., 2008). Because proline biosynthesis is a reductive process, both P5CS1 and P5CR require NADPH that regenerates $NADP^+$. The upregulation of the proline biosynthesis pathway under drought might contribute to maintaining the $NADP^+$ pool to sustain photosynthesis under stress conditions (De Ronde et al., 2004; Sharma et al., 2011). The proline degradation after stress release also presents numerous functions, including cellular signaling and stress recovery (Kishor et al., 2014). Our study showed that stress recovery was higher in NIL-143 compared to Scarlett (Figure 5). Since proline accumulation was

induced faster in NIL-143 than Scarlett during stress conditions, this might have resulted in greater protection of the cellular structure and macro-molecules and, thus, higher stress recovery.

Because NIL-143 surpassed Scarlett concerning stress tolerance and recovery, we evaluated the yield-related characteristics of NIL-143 and Scarlett in field drought conditions. Under field conditions, Scarlett accumulated 24% lower proline in the leaves compared to NIL-143 (Supporting Information: Figure S9). In addition, *QPro.S42-1H* ILs accumulated more proline in the spikes, and the spike abortion was significantly reduced under drought stress (Frimpong, Windt, et al., 2021). In the present study, the drought stress-induced reduction in yield attributing traits such as grain numbers per ear, grain weight per plant, harvest index, and thousand-grain weight, in particular, were higher in Scarlett compared with NIL-143 (Figure 7a,b and Supporting Information: Figures S11C,E). Blum (2017) reported that osmotic adjustment is one of the critical determinants of crop production under stressful environments. Previous studies have found a positive correlation between the osmotic adjustment capacity and grain yield in barley (Blum et al., 1999; González et al., 2008). NIL-143 showed a higher transpiration rate and stomatal conductance compared to Scarlett, maintaining 10% higher RWC and less negative leaf water potential under drought stress conditions (Frimpong, Anokye, et al., 2021) than Scarlett, which indicates a better osmotic adjustment in NIL-143.

## 5 | CONCLUSION

The present study demonstrated that the *P5CS1* promoter of high proline accumulating ISR42-8 harbors 130 predicted *cis*-elements that belong to 68 different families, including ABRE and related elements, MYB binding factors, NAC binding factors, DRE, CAATBOX 1, HEXAMERATH4 and WRKY boxes. The promoter variations were detected, especially across ABRE, MYB-binding motifs, HEXAMER-ATH4, PRECONSCRHSP70A and CAAT box among the diverse barley genotypes. The variation at these motifs was correlated to differences in the transcriptional activation of *P5CS1* and subsequent proline accumulation in selected haplotypes of barley. Further, the study provides necessary evidence on the significance of the *P5CS1* allele from wild barley ISR42-8 on drought tolerance in cultivated barley. We found that proline accumulation was enhanced in NIL-143 compared to Scarlett under drought conditions. As the significance of proline towards stress tolerance and recovery is well documented, the adaptive superiority of NIL-143 might also be linked to its proline phenotype. However, it has also been shown that proline accumulation in the leaf and the partitioning to other organs and turnover of proline are essential for proline-mediated drought tolerance (Sharma et al., 2011). In a previous study, we demonstrated that the NIL-143 accumulates higher proline in the roots than Scarlett (Frimpong, Anokye, et al., 2021), indicating the efficient partitioning of proline from the source (leaf) to the sink (root). Therefore, NIL-143 is an excellent genetic material for exploring the mechanistic process of

proline-mediated osmoregulation, redox balance, photosynthetic adjustments, and cellular signaling during drought stress.

## CONFLICT OF INTEREST

The authors declare no conflict of interest.

## DATA AVAILABILITY STATEMENT

The data that support the findings of this study are openly available in zenodo. org at https://zenodo.org/record/6988553.

## ORCID

Alexander Fendel http://orcid.org/0000-0001-6606-657X

Ali A. Naz https://orcid.org/0000-0002-0382-2128

## REFERENCES

Abrahám, E., Hourton-Cabassa, C., Erdei, L. & Szabados, L. (2010) Methods for determination of proline in plants. *Methods in Molecular Biology*, 639, 317–331.

Aleksza, D., Horváth, G.V., Sándor, G. & Szabados, L. (2017) Proline accumulation is regulated by transcription factors associated with phosphate starvation. *Plant Physiology*, 175, 555–567.

Barnabás, B., Jäger, K. & Fehér, A. (2008) The effect of drought and heat stress on reproductive processes in cereals. *Plant, Cell and Environment*, 31, 11–38.

Bartels, D. & Sunkar, R. (2005) Drought and salt tolerance in plants. *Critical Reviews in Plant Sciences*, 24, 23–58.

Bates, L.S., Waldren, R.P. & Teare, I.D. (1973) Rapid determination of free proline for water-stress studies. *Plant and Soil*, 39, 205–207.

Biłas, R., Szafran, K., Hnatuszko-Konka, K. & Kononowicz, A.K. (2016) Cis-regulatory elements used to control gene expression in plants, *Plant Cell, Tissue Organ Cult*, 127, pp. 269–287. Available from: http://link.springer.com/10.1007/s11240-016-1057-7

Blum, A. (2017) Osmotic adjustment is a prime drought stress adaptive engine in support of plant production. *Plant, Cell and Environment*, 40, 4–10.

Blum, A., Zhang, J. & Nguyen, H.T. (1999) Consistent differences among wheat cultivars in osmotic adjustment and their relationship to plant production. *Field Crops Research*, 64, 287–291.

Carter, G.A. (1994) Ratios of leaf reflectances in narrow wavebands as indicators of plant stress. *International Journal of Remote Sensing*, 15, 517–520.

Chattopadhyay, M.K., Kern, R., Mistou, M.Y., Dandekar, A.M., Uratsu, S.L. & Richarme, G. (2004) The chemical chaperone proline relieves the thermosensitivity of a dnaK deletion mutant at 42°C. *Journal of Bacteriology*, 186, 8149–8152.

Chaves, M. & Davies, B. (2010) Drought effects and water use efficiency: improving crop production in dry environments. *Functional Plant Biology*, 37, 37.

Dziwornu, A.K., Shrestha, A., Matthus, E., Ali, B., Wu, L.B. & Frei, M. (2018) Responses of contrasting rice genotypes to excess manganese and their implications for lignin synthesis. *Plant Physiology and Biochemistry*, 123, 252–259. Available from: https://doi.org/10.1016/j.plaphy.2017.12.018

Fedina, I.S., Grigorova, I.D. & Georgieva, K.M. (2003) Response of barley seedlings to UV-B radiation as affected by NaCl. *Journal of Plant Physiology*, 160, 205–208.

Frimpong, F., Anokye, M., Windt, C.W., Naz, A.A., Frei, M. & Dusschoten, D. et al. (2021) Proline-mediated drought tolerance in the barley (*Hordeum vulgare* L.) isogenic line is associated with lateral root growth at the early seedling stage. *Plants*, 10(10), 2177.

Frimpong, F., Windt, C.W., Dusschoten, D., van Naz, A.A., Frei, M. & Fiorani, F. (2021) A wild allele of pyrroline-5-carboxylate synthase1 leads to proline accumulation in spikes and leaves of barley contributing to improved performance under reduced water availability. *Frontiers of Plant Science*, 12, 633448.

Gadallah, M.A.A. (1999) Effects of proline and glycinebetaine on *Vicia faba* responses to salt stress. *Biologia Plantarum*, 42, 249–257.

González, A., Martín, I. & Ayerbe, L. (2008) Yield and osmotic adjustment capacity of barley under terminal water-stress conditions. *Journal of Agronomy and Crop Science*, 194, 81–91.

Hare, P.D., Cress, W.A. & Van Staden, J. (1998) Dissecting the roles of osmolyte accumulation during stress. *Plant, Cell and Environment*, 21, 535–553.

Hari, V., Rakovec, O., Markonis, Y., Hanel, M. & Kumar, R. (2020) Increased future occurrences of the exceptional 2018–2019 Central European drought under global warming. *Scientific Reports*, 10, 1–10. Available from: https://doi.org/10.1038/s41598-020-68872-9

Hassine, A.B., Ghanem, M.E., Bouzid, S. & Lutts, S. (2008) An inland and a coastal population of the Mediterranean xero-halophyte species *Atriplex halimus* L. differ in their ability to accumulate proline and glycinebetaine in response to salinity and water stress. *Journal of Experimental Botany*, 59, 1315–1326.

Hobo, T., Asada, M., Kowyama, Y. & Hattori, T. (1999) ACGT-containing abscisic acid response element (ABRE) and coupling element 3 (CE3) are functionally equivalent. *The Plant Journal*, 19, 679–689.

Hochberg, U., Degu, A., Toubiana, D., Gendler, T., Nikoloski, Z., Rachmilevitch, S. et al. (2013) Metabolite profiling and network analysis reveal coordinated changes in grapevine water stress response. *BMC Plant Biology*, 13, 13.

Kavi Kishor, P.B., Sangam, S., Amrutha, R.N., Sri Laxmi, P., Naidu, K.R. & Rao, K.R.S.S. et al. (2005) Regulation of proline biosynthesis, degradation, uptake and transport in higher plants: its implications in plant growth and abiotic stress tolerance. *Current Science*, 88, 424–438.

Kim, W., Iizumi, T. & Nishimori, M. (2019) Global patterns of crop production losses associated with droughts from 1983 to 2009. *Journal of Applied Meteorology and Climatology*, 58, 1233–1244.

Kishor, P.B.K., Sreenivasulu, N., Kavi Kishor, P.B., Sreenivasulu, N., Kishor, P.B.K., Sreenivasulu, N. et al. (2014) Is proline accumulation per se correlated with stress tolerance or is proline homeostasis a more critical issue? *Plant, Cell and Environment*, 37, 300–311.

Kiyosue, T., Yoshiba, Y., Yamaguchi-Shinozaki, K. & Shinozaki, K. (1996) A nuclear gene encoding mitochondrial proline dehydrogenase, an enzyme involved in proline metabolism, is upregulated by proline but downregulated by dehydration in Arabidopsis. *The Plant Cell*, 8, 1323–1335.

Koua, A.P., Oyiga, B.C., Baig, M.M., Léon, J. & Ballvora, A. (2021) Breeding driven enrichment of genetic variation for key yield components and grain starch content under drought stress in winter wheat. *Frontiers of Plant Science*, 12, 1–18.

Livak, K.J. & Schmittgen, T.D. (2001) Analysis of relative gene expression data using real-time quantitative PCR and the 2(-Delta Delta C (T))$2^{-\Delta\Delta C_t}$ method. *Methods*, 25, 402–408.

Main, R., Cho, M.A., Mathieu, R., O'Kennedy, M.M., Ramoelo, A. & Koch, S. (2011) An investigation into robust spectral indices for leaf chlorophyll estimation. *ISPRS Journal of Photogrammetry and Remote Sensing*, 66, 751–761. Available from: https://doi.org/10.1016/j.isprsjprs.2011.08.001

Le Maire, G., François, C. & Dufrêne, E. (2004) Towards universal broad leaf chlorophyll indices using PROSPECT simulated database and hyperspectral reflectance measurements. *Remote Sensing of the Environment*, 89, 1–28.

Mittler, R. (2002) Oxidative stress, antioxidants and stress tolerance. *Trends in Plant Science*, 7, 405–410.

Muzammil, S. (2018) *Genetic dissection of shoot traits and proline content under control and drought conditions in barley*. PhD Thesis. p. 55. Available at: http://hss.ulb.uni-bonn.de/2018/5081/5081.pdf [Accessed 1st February 2021].

Muzammil, S., Shrestha, A., Dadshani, S., Pillen, K., Siddique, S., Léon, J. et al. (2018) An ancestral allele of pyrroline-5-carboxylate synthase1 promotes proline accumulation and drought adaptation in cultivated barley. *Plant Physiology*, 178, 771–782.

Nakashima, K., Ito, Y. & Yamaguchi-Shinozaki, K. (2009) Transcriptional regulatory networks in response to abiotic stresses in arabidopsis and grasses. *Plant Physiology*, 149, 88–95. Available from: http://www.plantphysiol.org/cgi/doi/10.1104/pp.108.129791

Nounjan, N. & Theerakulpisut, P. (2012) Effects of exogenous proline and trehalose on physiological responses in rice seedlings during salt-stress and after recovery. *Plant, Soil Environment* 58, 309–315. Available from: https://doi.org/10.1016/j.jplph.2012.01.004

R Core Team. (2020) *R: A Language and Environment for Statistical Computing*. Vienna, Austria: R Foundation for Statistical Computing. Available at: https://www.R-project.org/ [Accessed 1st September 2021].

Rajendrakumar, C.S.V., Reddy, B.V.B. & Reddy, A.R. (1994) Proline-Protein interactions: protection of structural and functional integrity of M4 lactate dehydrogenase. *Biochemical and Biophysical Research Communications*, 201, 957–963. Available from: https://linkinghub.elsevier.com/retrieve/pii/S0006291X84717955

De Ronde, J.A., Cress, W.A., Krüger, G.H.J., Strasser, R.J. & Van Staden, J. (2004) Photosynthetic response of transgenic soybean plants, containing an Arabidopsis P5CR gene, during heat and drought stress. *Journal of Plant Physiology*, 161, 1211–1224.

Sharkey, T.D. (2016) What gas exchange data can tell us about photosynthesis, *Plant Cell Environment*, 39, pp. 1161–1163. Available at: https://doi.org/10.1111/pce.12641

Sharkey, T.D., Bernacchi, C.J., Farquhar, G.D. & Singsaas, E.L. (2007) Fitting photosynthetic carbon dioxide response curves for C3 leaves. *Plant, Cell and Environment*, 30, 1035–1040.

Sharma, S. & Verslues, P.E. (2010) Mechanisms independent of abscisic acid (ABA) or proline feedback have a predominant role in transcriptional regulation of proline metabolism during low water potential and stress recovery. *Plant, Cell and Environment*, 33, 1838–1851.

Sharma, S., Villamor, J.G. & Verslues, P.E. (2011) Essential role of tissue-specific proline synthesis and catabolism in growth and redox balance at low water potential. *Plant Physiology*, 157, 292–304.

Shen, Q., Zhang, P. & Ho, T.H. (1996) Modular nature of abscisic acid (ABA) response complexes: composite promoter units that are necessary and sufficient for ABA induction of gene expression in barley. *The Plant Cell*, 8, 1107–1119.

Shrestha, A., Cudjoe, D.K., Kamruzzaman, M., Siddique, S., Fiorani, F., Léon, J. et al. (2021) Abscisic acid-responsive element binding transcription factors contribute to proline synthesis and stress adaptation in Arabidopsis. *Journal of Plant Physiology*, 261, 153414.

Siddiqui, M.N., Teferi, T.J., Ambaw, A.M., Gabi, M.T., Koua, P., Léon, J. et al. (2021) New drought-adaptive loci underlying candidate genes on wheat chromosome 4B with improved photosynthesis and yield responses. *Physiologia Plantarum*, 173, 2166–2180.

Singh, D.K., Sale, P.W.G., Pallaghy, C.K. & Singh, V. (2000) Role of proline and leaf expansion rate in the recovery of stressed White clover leaves with increased phosphorus concentration. *New Phytologist*, 146, 261–269.

Sripinyowanich, S., Klomsakul, P., Boonburapong, B., Bangyeekhun, T., Asami, T., Gu, H. et al. (2013) Exogenous ABA induces salt tolerance in indica rice (*Oryza sativa* L.): the role of OsP5CS1 and OsP5CR gene expression during salt stress. *Environmental and Experimental Botany*, 86, 94–105. Available from: https://doi.org/10.1016/j.envexpbot.2010.01.009

Szabados, L. & Savouré, A. (2010) Proline: a multifunctional amino acid, *Trends in Plant Science*, 15, pp. 89–97. Available from: https://doi.org/10.1111/j.0960-7412.1997.00557.x

Székely, G., Abrahám, E., Cséplö, A., Rigó, G., Zsigmond, L., Csiszár, J. et al. (2008) Duplicated P5CS genes of Arabidopsis play distinct roles in stress regulation and developmental control of proline biosynthesis. *The Plant Journal*, 53, 11–28.

Trenberth, K.E., Dai, A., Schrier, G., Van Der Jones, P.D., Barichivich, J. & Briffa, K.R. et al. (2014) Global warming and changes in drought. *Nature Climate Change*, 4, 17–22.

Trovato, M., Funck, D., Forlani, G., Okumoto, S. & Amir, R. (2021) Editorial: amino acids in plants: regulation and functions in development and stress defense. *Frontiers of Plant Science*, 12, 1–5.

Uddling, J., Gelang-Alfredsson, J., Piikki, K. & Pleijel, H. (2007) Evaluating the relationship between leaf chlorophyll concentration and SPAD-502 chlorophyll meter readings. *Photosynthesis Research*, 91, 37–46.

Verslues, P.E., Lasky, J.R., Juenger, T.E., Liu, T.W. & Nagaraj Kumar, M. (2014) Genome-wide association mapping combined with reverse genetics identifies new effectors of low water potential-induced proline accumulation in Arabidopsis. *Plant Physiology*, 164, 144–159.

Verslues, P.E. & Sharp, R.E. (1999) Proline accumulation in maize (*Zea mays* L.) primary roots at low water potentials. II. metabolic source of increased proline deposition in the elongation zone. *Plant Physiology*, 119, 1349–1360.

Xia, Y., Li, R., Bai, G., Siddique, K.H.M., Varshney, R.K., Baum, M. et al. (2017) Genetic variations of HvP5CS1 and their association with drought tolerance related traits in barley (*Hordeum vulgare* L.). *Scientific Reports*, 7, 1–10. Available from: https://doi.org/10.1038/s41598-017-08393-0

Yoshida, T., Fujita, Y., Maruyama, K., Mogami, J., Todaka, D., Shinozaki, K. et al. (2015) Four Arabidopsis AREB/ABF transcription factors function predominantly in gene expression downstream of SnRK2 kinases in abscisic acid signalling in response to osmotic stress. *Plant, Cell and Environment*, 38, 35–49.

## SUPPORTING INFORMATION

Additional supporting information can be found online in the Supporting Information section at the end of this article.